Available online at www.sciencedirect.com
SCIENCE DIRECT
Journal of Catalysis 232 (2005) 96–101
JOURNAL OF CATALYSIS
www.elsevier.com/locate/jcat

Alkali (earth)-doped Au/Al_2O_3 catalysts for the total oxidation of propene

Andreea Catalina Gluhoi [a], Nina Bogdanchikova [b], Bernard E. Nieuwenhuys [a,*]

[a] *Department of Heterogeneous Catalysis and Surface Chemistry, Leiden Institute of Chemistry, Leiden University, P.O. Box 9502, 2300 RA Leiden, The Netherlands*

[b] *Centro de Ciencias de la Materia Condensada-UNAM, Km. 107, Carretera Tijuana-Ensenada, 22800, Ensenada, Baja California, Mexico*

Received 19 January 2005; revised 15 February 2005; accepted 18 February 2005

Available online 7 April 2005

Abstract

The addition of alkali (earth) metal oxides (MO_x, with M = Li, Rb, Mg, or Ba) is beneficial for the performance of Au/Al_2O_3 catalysts in the total oxidation of propene (C_3H_6). The effect of the MO_x additives on the microstructure and nature of Au/Al_2O_3 catalyst was investigated by X-ray diffraction (XRD), high-resolution transmission electron microscopy (HRTEM), total surface area (BET), and diffuse reflectance ultraviolet visible spectroscopy (DR-UV/vis). It is found that MO_x induces a decrease in the size of gold particles and stabilizes them against sintering. In turn, a direct dependence of the catalytic performance on the size of the gold particles is found. The role of the additives is that of a structural promoter and not a chemical promoter.

Keywords: Gold; Additives; Alkali (earth) metal oxides; Promoter; Propene oxidation

1. Introduction

In the last decade there has been a growing interest in catalysis by gold. It is now accepted that the catalytic behavior of gold nanoparticles deposited on an appropriate support differs significantly from that of massive gold. In particular, CO oxidation in the presence (PROX) or absence of hydrogen has attracted considerable attention [1–6]. A few studies have been devoted to the total oxidation of volatile organic compounds (VOCs) over Au/Al_2O_3 and Au/CeO_2 [7,8]. Recently we examined the influence of CeO_x, MnO_x, FeO_x, and CoO_x on the catalytic activity of Au/Al_2O_3 [9] for the total oxidation of propene as one of the hydrocarbons that appear in automotive emission, and we showed that $Au/CeO_x/Al_2O_3$ is an efficient catalyst for this reaction. The present study deals with the effect induced by alkali (earth) metal oxides on the catalytic performance of Au/Al_2O_3 in C_3H_6 oxidation.

According to the literature, the addition of alkali (earth) metal oxides (MO_x) may be beneficial for or detrimental to the catalyst performance. For gold catalysis, it has been reported that the addition of Li_2O to Au/Al_2O_3 is beneficial for N_2O reduction by H_2 [10]. The promotion effect of K, Cs, and Ba addition on Fe- and Ru-based catalysts for NH_3 synthesis is extensively described in the literature [11–14] and is relatively well understood. Low levels of alkali dopants are beneficial for the performance of MoO_x-based catalysts toward C_3H_8 oxidative dehydrogenation (ODH) [15]. Calcium was reported to act either as a promoter (low Ca/Cr ratios) or a poison (higher Ca/Cr ratios) for chromium oxide catalysts supported on Al_2O_3 in the ODH of isobutene [16]. A poison effect of alkali ions has been reported, for example, in acetonitrile hydrogenation [17] and the deuterium exchange reaction between ammonia and hydrogen [18].

In the study described in the present paper, the singly promoted systems $Au/Li_2O/Al_2O_3$, $Au/Rb_2O/Al_2O_3$, $Au/MgO/Al_2O_3$, and $Au/BaO/Al_2O_3$ were prepared by homogeneous deposition precipitation. Various techniques, such as XRD, HRTEM, BET, and DR-UV/vis, were used to study the structural properties of the catalysts. Finally, the physico-

* Corresponding author.
E-mail address: b.nieuwe@chem.leidenuniv.nl (B.E. Nieuwenhuys).

0021-9517/$ – see front matter
doi:10.1016/j.jcat.2005.02.016

chemical characteristics of the catalysts are discussed in relation to the catalytic performance in propene oxidation.

2. Experimental procedures

2.1. Catalyst preparation

Mixed oxides (MO_x/Al_2O_3) were prepared by vacuum impregnation of γ-Al_2O_3 (Engelhard, $S_{BET} = 275\ m^2\ g^{-1}$) with the corresponding nitrates of Li, Rb, Mg, and Ba (Aldrich; > 99.9% purity). After drying for at least 16 h at 80 °C in static air, the samples were subjected to calcination in O_2 flow at 350 °C for 2 h. The prepared mixed oxides typically have an M/Al atomic ratio of 1:15.

Gold was added to Al_2O_3 or MO_x/Al_2O_3 via homogeneous deposition-precipitation (HDP), with urea as a precipitating agent [10]. The gold precursor used was $HAuCl_4 \cdot 3H_2O$ (Aldrich; 99.99%). The support (either pure alumina or MO_x/Al_2O_3), the corresponding solution of $HAuCl_4 \cdot 3H_2O$, water, and urea in excess were warmed to 80 °C with vigorous stirring. The final pH of the solution was 8.5. The advantage of this method is that, because of the slow decomposition of urea, gold deposition takes place mainly on the surface of the support. Moreover, this preparation method ensures rather reproducible results regarding two important aspects: gold loading and gold particle size.

2.2. Catalyst characterization

Atomic absorption spectroscopy (AAS) was used to determine the exact gold loading of the as-prepared gold-based catalysts. The experiments were carried out with a Perkin–Elmer 3100 apparatus with an air/acetylene flame. A small amount of the catalyst was dissolved in aqua regia ($3HCl:HNO_3$), and the solution was diluted with demineralized water before the analysis was performed.

The BET surface area was measured by physical adsorption of N_2 at −196 °C with an automatic Qsurf M1 apparatus (Thermo Finnigan). Before each measurement the catalyst was degassed for 2 h in helium at 200 °C to remove impurities.

XRD measurements were carried out with a Philips Goniometer (PW 1050/25) diffractometer equipped with a PW Cu 2103/00 X-ray tube operated at 50 kV and 40 mA. The average gold particle size was estimated from XRD line broadening with the Scherrer equation. The spectra were recorded between $2\theta = 20°$ and 60 °.

HRTEM measurements were performed with a JEOL 2010 microscope with a point-to-point resolution better than 0.19 nm. The sample was mounted on a carbon polymer-supported copper micro-grid. A few droplets of a suspension of the ground catalyst in isopropyl alcohol were placed on the grid, followed by drying at ambient conditions. The average gold particles and the particle size distribution were determined from a count of at least 250–300 particles.

For DR-UV/vis experiments a Perkin–Elmer spectrometer (Lambda 900) was used, and the air-exposed samples were analyzed in the range of λ between 200 and 850 nm.

2.3. Catalytic activity measurements

Propene (C_3H_6) oxidation was carried out in a flow reactor. Before each experiment, the catalyst (0.2 g) was activated in situ at 300 °C for 30 min with the use of 4 vol% H_2/He. The feed gases were controlled with mass flow controllers (Bronkhorst) and set to a total flow of 30 ml min^{-1}. The reaction mixture contained a large excess of oxygen (about 9 times more oxygen). Each experiment consisted of at least two heating-cooling cycles, to monitor catalyst deactivation processes. The outlet gas stream was analyzed every minute with either a gas chromatograph (Chrompack CP-9001) or a quadrupole mass spectrometer (Spectra). The GC was equipped with a flame ionization detector (FID), a Hayesep N column (50 °C), and a methanizer.

3. Results and discussion

The structural characteristics of Au/Al_2O_3 and $Au/MO_x/Al_2O_3$ (M = Li, Rb, Mg, Ba) are summarized in Table 1. The gold loading (AAS results) varies between 3.5 wt% ($Au/Rb_2O/Al_2O_3$) and 4.2 wt% ($Au/MgO/Al_2O_3$). As summarized in Table 1, the BET total surface area is not drastically affected by gold deposition. The maximum decrease observed was 20% and was found for $Au/MgO/Al_2O_3$. It is possible that during vacuum impregnation and the subsequent deposition precipitation steps, some of the pores of alumina were blocked.

XRD analysis revealed for all catalysts the diffraction pattern of metallic gold. The average gold particle sizes are summarized in Table 1 as d^{a}_{Au}. Generally, very small gold particles were found; the largest particles (4.3 nm) were present on Au/Al_2O_3. However, it should be noted that XRD cannot detect small crystallites or amorphous phases. Because of the relatively low loading of the additives (M/Al atomic ratio of 1:15), the MO_x phase was not detected for all of the MO_x used. This is most probably due to a rather amorphous phase of MO_x, as a result of the low loading. The smaller values of d_{Au} for the MO_x-containing catalysts lead us to the conclusion that these additives have a beneficial effect on the stabilization of small Au particles. In fact, the positive effect of Li_2O [10] and some alkali-earth metal oxides [19,20] on the gold particle size has already been reported in the literature.

Some of the catalysts were studied in more detail by HRTEM; the data have been included in Table 1 as d^{b}_{Au}. In agreement with the XRD data, the gold particles were rather large for Au/Al_2O_3 (5.2 nm) and very small (below 3.0 nm) for $Au/Rb_2O/Al_2O_3$ and $Au/BaO/Al_2O_3$. A typical graph of the particle size distribution is presented in Fig. 1 for Au/Al_2O_3, $Au/Rb_2O/Al_2O_3$, and $Au/BaO/Al_2O_3$.

Table 1
Physico-chemical properties of the alkali (earth) metal oxides-promoted gold-based catalysts by means of: AAS, BET, XRD, HRTEM and the full width at the half maximum FWHM obtained from DR-UV/vis measurements

Catalyst	Au (wt%)	S_{BET} ($m^2\ g^{-1}$)	d^a_{Au} (nm)	d^b_{Au} (nm)	d^c_{Au} (nm)	S_{Au}[a] ($m^2\ g^{-1}$)	FWHM (nm)
Au/Al_2O_3	4.1 ± 0.1	260 ± 5	4.3 ± 0.1	5.2 ± 0.3	4.5 ± 0.2	1.5	71.1 ± 1.2
$Au/BaO/Al_2O_3$	3.6 ± 0.2	240 ± 8	–[b]	1.5 ± 0.2	–[b]	6.2	189.4 ± 1.2
$Au/MgO/Al_2O_3$	4.2 ± 0.1	224 ± 10	4.0 ± 0.1	n.m.	3.7 ± 0.2	n.m.	100.7 ± 3.4
$Au/Li_2O/Al_2O_3$	4.0 ± 0.3	278 ± 7	3.2 ± 0.1	3.0 ± 0.1	3.4 ± 0.1	2.5	86.4 ± 8.3
$Au/Rb_2O/Al_2O_3$	3.5 ± 0.1	294 ± 3	–[b]	2.6 ± 0.3	3.3 ± 0.1	3.6	164.5 ± 15
Al_2O_3	–	275 ± 5	–	–	–	–	–

d^a_{Au}: mean diameter of gold particles, as determined by XRD, fresh catalysts (as prepared, before the reaction test); d^b_{Au}: mean diameter of gold particles, as determined by HRTEM, fresh catalysts (as prepared, before the reaction test); d^c_{Au}: mean diameter gold particles, as determined by XRD, spent catalysts (after the reaction test); FWHM: the full width at the half maximum as determined by DR-UV/vis; n.m.: not measured.
[a] S_{Au}: gold surface area as determined by HRTEM.
[b] –: not detectable by XRD.

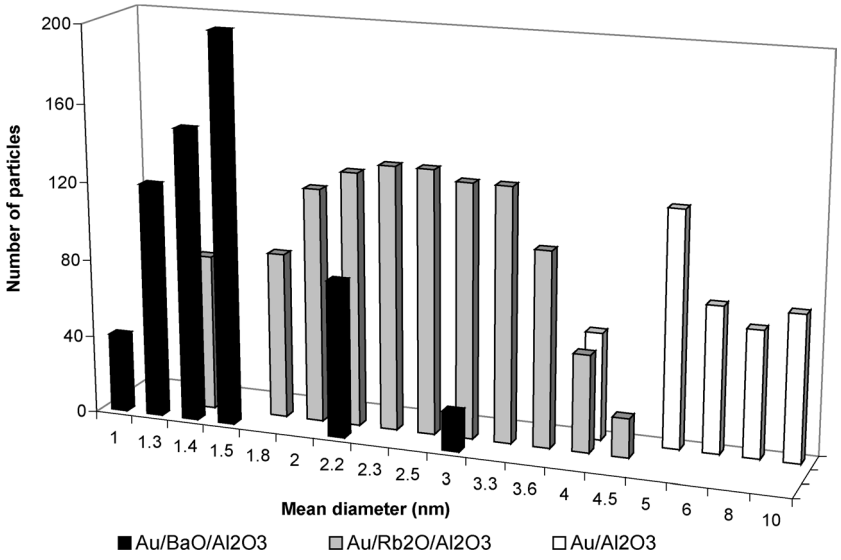

Fig. 1. Gold particle size distribution as determined by HRTEM for Au/Al_2O_3, $Au/Rb_2O/Al_2O_3$ and $Au/BaO/Al_2O_3$.

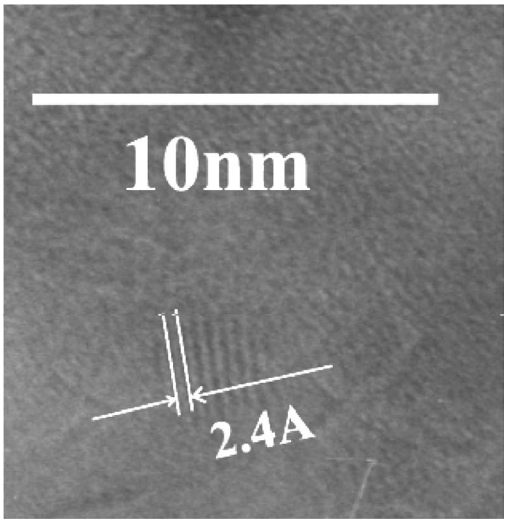

Fig. 2. HRTEM micrograph of $Au/Rb_2O/Al_2O_3$.

Clearly, there is a significant difference in the particle size distribution between the samples *with* or *without* MO_x additive. The growth of large gold particles at the expense of the smaller crystallites appears to be inhibited in the presence of alkali (earth) metal oxides. In addition, the lattice spacing of Au was visualized for $Au/Rb_2O/Al_2O_3$ by HRTEM. The corresponding micrograph is shown in Fig. 2, and the lattice space measured is 2.4 Å. This is, within experimental error, the (111) reflection of metallic Au (JCPD powder diffraction data base reports 2.355 Å [21]). No other reflections corresponding to metallic gold were detected for any of the samples.

The shape of the gold particles, as visualized by HRTEM, was spherical, and no other shapes were seen. However, shapes other than spherical cannot be excluded, since it is known that with a decrease in the size of the Au particles, other morphologies are likely to be formed. According to other studies, the number of low coordinated atoms is also related to the size of the Au particles [22]. Smaller Au particles are assumed to have an increased number of low coordinated atoms that are highly active toward the ac-

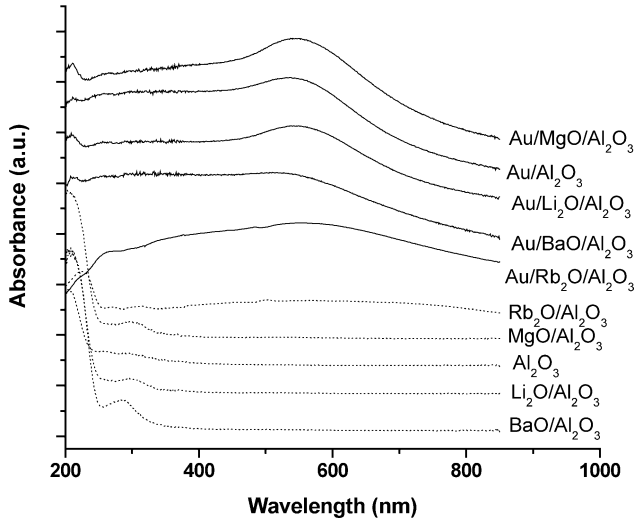

Fig. 3. DR-UV/vis optical spectra of different gold-based catalysts and the corresponding supports.

tivation of molecules [22–24]. Hence, it is expected that $Au/BaO/Al_2O_3$ and $Au/Rb_2O/Al_2O_3$ in particular exhibit an increased number of low coordinated sites that are able to activate reactants.

The chemical state of gold was also studied by DR-UV/vis. Fig. 3 shows the optical spectra, including those of the supports. The surface plasmon absorption band, characteristic of small Au^0 species, was found, for all of the catalysts, with a maximum between 500 and 600 nm. The values of the full width at half-maximum (FWHM), as estimated from the peak shape of the optical spectra, are also summarized in Table 1. The FWHM value decreases from 189.4 nm ($Au/BaO/Al_2O_3$, very small particles) to 71.1 nm (Au/Al_2O_3, large gold particles), in line with the variation of the size of gold particles. However, the relation (between the mean particle diameter, the peak position, and the FWHM) is also influenced by the surrounding environment and the interaction between the gold particles and the support [25,26].

The catalytic performance of the gold-based catalysts is presented in Fig. 4 in terms of the temperature needed to reach 50% C_3H_6 conversion. It should be mentioned that propene conversion over γ-Al_2O_3 did not exceed 22% at the highest temperature used. In addition, the mixed supports MO_x/Al_2O_3 (M = Li, Rb, Mg, or Ba) have also been tested in propene oxidation and were found to be negligibly active under the reaction conditions used in this study. The only C-containing molecule obtained as a product is CO_2. The introduction of alkali (earth) metal oxides definitely improves the catalytic performance of Au/Al_2O_3 over the whole temperature range. Thus, the $T_{50\%}$ decreases from 365 °C (Au/Al_2O_3) to 290 °C ($Au/BaO/Al_2O_3$). Contrary to reactions where alkali metal oxides act as poison, such as the selective reduction of NO with NH_3 over TiO_2-supported V_2O_5 [27], or the H–D isotopic exchange reaction between OH groups of H-ZSM-5 and D_2 in the gas phase [28], their presence is beneficial for gold-based catalysts in propene oxidation.

The change in the gold particle size during the catalytic cycle was followed by XRD; the results are summarized in Table 1 as d^c_{Au}. In general the gold particles do not sinter significantly during the reaction test. However, the gold crystallites of the catalysts that contain an additive seem more stable against sintering.

The variation of the temperature of 50% conversion with the average gold particle size of gold-based catalysts in

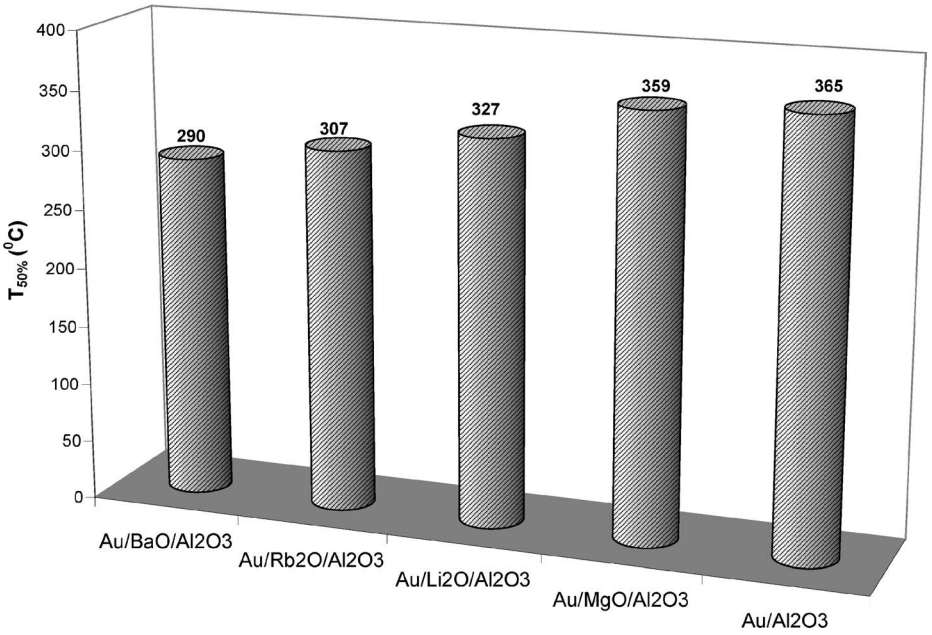

Fig. 4. Catalytic activity performance expressed in terms of $T_{50\%}$ (the temperature needed to reach 50% propene conversion) of various gold-based catalysts (C_3H_6:O_2 ratio = 1:9).

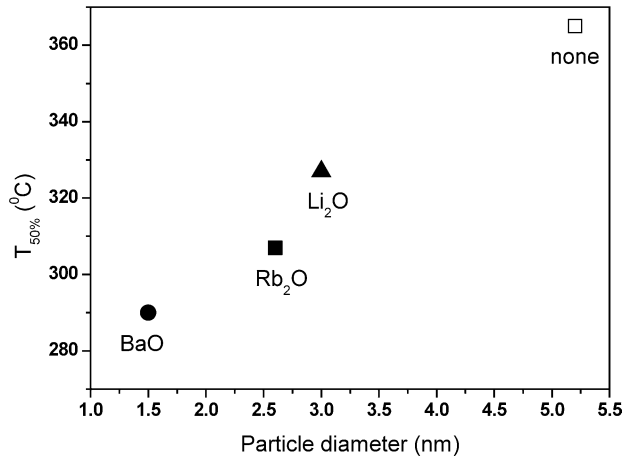

Fig. 5. Temperature needed for 50% C_3H_6 conversion versus the average gold particle size (HRTEM) of unpromoted (□) and Li_2O (▲)-, Rb_2O (■)- and BaO (●)-promoted Au/Al_2O_3 catalysts.

C_3H_6 oxidation is shown in Fig. 5. The data are given for each sample characterized by HRTEM. The variation of $T_{50\%}$ is related to the size of the Au particles because the mixed support itself is hardly active toward propene oxidation. Hence, a direct correlation exists between $T_{50\%}$ and d^{b}_{Au}, and an increase in d^{b}_{Au} results in an increase in $T_{50\%}$.

The variation of the specific reaction rate, r, defined as the amount of C_3H_6 (moles) transformed over the amount of gold (moles) per second, was calculated for the various catalysts at different reaction temperatures. The results are summarized in Table 2 for a reaction temperature of 260 °C. The specific reaction rate varies between 1.38×10^{-6} ((moles C_3H_6) (moles Au)$^{-1}$ s^{-1}) for Au/Al_2O_3 and 8.1×10^{-6} ((moles C_3H_6) (moles Au)$^{-1}$ s^{-1}) for $Au/BaO/Al_2O_3$. The addition of BaO to Au/Al_2O_3 produces a sixfold increase in the reaction rate. The values for the other gold-containing catalysts are between these limits. The ranking of the catalysts based on r values is $Au/Al_2O_3 < Au/Li_2O/Al_2O_3 < Au/Rb_2O/Al_2O_3 < Au/BaO/Al_2O_3$, and it fits with the trend observed from Figs. 4 and 5. The variation in the specific reaction rate is clearly affected by the change in the size of the Au particles. As a direct consequence of the smaller gold particle size in the presence of an alkali (earth) metal oxide, the metallic surface area as estimated from HRTEM is strongly increased by the addition of the oxides (see Table 1). A larger metallic surface area/smaller average Au particle size is beneficial for the catalytic performance, if the noble metal is the active component on the catalyst.

The question is, what is the role of the additives? Is their action only related to the effect on the particle size of gold (as structural promoters), or can they also play another role in the reaction, as chemical promoters, such as in NH_3 synthesis?

It is well established that oxides with redox properties (CeO_2, Fe_2O_3, and other transition-metal oxides, CuO, etc. [1,2,9,10,29]) have a large effect on the catalytic activity of gold-based catalysts. Alkali (earth) metal oxides do not have any ability to supply active oxygen; therefore an explanation in terms of a redox mechanism can be excluded.

Table 2
The specific reaction rate at 260 °C and the apparent activation energy of the gold-based catalysts tested in C_3H_6 oxidation (total flow: 30 ml min^{-1}, reactant ratio $C_3H_6/O_2 = 1/9$ vol)

Catalyst	$r \times 10^6$ ((moles C_3H_6) (moles Au)$^{-1}$ s^{-1})	E_a (kJ mol^{-1})
Al_2O_3	–	90 ± 2
Au/Al_2O_3	1.38	67 ± 3
$Au/MgO/Al_2O_3$	1.86	61 ± 4
$Au/Li_2O/Al_2O_3$	3.16	65 ± 3
$Au/Rb_2O/Al_2O_3$	6.93	65 ± 2
$Au/BaO/Al_2O_3$	8.01	66 ± 2

To elucidate the role of the additives on the catalytic performance of the gold-based catalysts, we have calculated the apparent activation energy at a conversion ranging from 0.05 to 0.2. The results are tabulated in Table 2, last column. First, it is found that E_a decreases after the addition of gold to Al_2O_3, from ca. 90 kJ mol^{-1} (Al_2O_3) to 67 kJ mol^{-1} (Au/Al_2O_3), indicating that gold is the active species in C_3H_6 oxidation. Second, it is found that the presence/nature of the alkali (earth) metal oxide does not significantly change the apparent activation energy. The negligible effect of MO_x addition (M = Li, Rb, Mg, Ba) on E_a suggests that the presence of MO_x does not create new reaction paths for C_3H_6 oxidation.

For ammonia synthesis, the role of alkali metal oxides (K_2O, Cs_2O) on Fe- and Ru-based catalysts is well established, and they act as chemical promoters by lowering the N_2 dissociation barrier [11,12,14,30]. A complete different situation was found for the gold-based catalysts presented here. The experimental data prove that the role of MO_x is first that of a stabilizer for small gold particles (XRD and HRTEM data), and no direct effect on the chemical process could be detected by means of E_a. Thus, the role of alkali (earth) metal oxides is rather to increase the concentration of the Au active sites, without creating new reaction pathways. These additives appear to act as structural promoters.

4. Conclusions

Au/Al_2O_3 and alkali (earth) metal oxide-promoted Au/Al_2O_3 catalysts have been prepared, characterized, and tested in the total oxidation of C_3H_6.

- The promoted Au/Al_2O_3 catalysts of very small gold particles are much more active than unpromoted gold-based catalyst in the total oxidation of propene.
- The apparent activation energy, E_a, of Au/Al_2O_3 and $Au/MO_x/Al_2O_3$ catalysts shows that the additives (Li_2O, Rb_2O, MgO, and BaO) are not directly responsible for the higher catalytic activity. Presumably, their

role is to increase the concentration of the Au active sites. The best promoting effect is obtained when BaO is used.

Acknowledgment

A.C.G. would like to express her gratitude to Dr. P. Marginean for fruitful discussions and to F. Ruiz Medina, E. Flores, J. Peralta, and M. Sainz for technical support. The Netherlands Organization for Scientific research (NWO) (grants NWO/CW 99037 and NWO #047.015.003) and CONACYT (42568-Q) and PAPIIT-UNAM (IN109003) Mexican grants are gratefully acknowledged for financial support.

References

[1] R.J.H. Grisel, B.E. Nieuwenhuys, J. Catal. 199 (2001) 48.
[2] R.J.H. Grisel, C.J. Weststrate, A.C. Gluhoi, B.E. Nieuwenhuys, Gold Bull. 35 (2002) 39, and references therein.
[3] M. Haruta, T. Kobayashi, N. Yamada, Chem. Lett. 2 (1987) 405.
[4] M. Haruta, S. Tsubota, T. Kobayashi, H. Kageyama, M.J. Genet, B. Delmon, J. Catal. 144 (1993) 175.
[5] S.D. Lin, M. Bollinger, M.A. Vannice, Catal. Lett. 17 (1993) 245.
[6] R.M.T. Sanchez, A. Ueda, K. Tanaka, M. Haruta, J. Catal. 168 (1997) 125.
[7] S. Minico, S. Scire, C. Crisafulli, R. Maggiore, S. Galvagno, Appl. Catal. B 28 (2000) 245.
[8] S. Scire, S. Minico, C. Crisafulli, C. Satriano, A. Pistone, Appl. Catal. B 40 (2003) 43.
[9] A.C. Gluhoi, N. Bogdanchikova, B.E. Nieuwenhuys, J. Catal. 229 (2005) 154.
[10] A.C. Gluhoi, M.A.P. Dekkers, B.E. Nieuwenhuys, J. Catal. 219 (2003) 197.
[11] Z. Kowalczyk, M. Krukowski, W. Rarog-Pilecka, D. Szmigiel, J. Zielinski, Appl. Catal. A 248 (2003) 67.
[12] Z. Kowalczyk, J. Sentek, S. Jodzis, M. Muhler, O. Hinrichsen, J. Catal. 169 (1997) 407.
[13] W. Rarog, Z. Kowalczyk, J. Sentek, D. Skladanowski, J. Zielinski, Catal. Lett. 68 (2000) 163.
[14] R.A. van Santen, J.W. Niemantsverdriet, Chemical Kinetics and Catalysis, Plenum Press, New York, 1995.
[15] R.B. Watson, U.S. Ozkan, J. Mol. Catal. A 194 (2003) 115.
[16] G. Neri, A. Pistone, S. De Rossi, E. Rombi, C. Milone, S. Galvagno, Appl. Catal. A 260 (2004) 75.
[17] M.J.F.M. Verhaak, A.J. van Dillen, J.W. Geus, Catal. Lett. 26 (1994) 37.
[18] P. Marginean, A. Olariu, Appl. Catal. A 165 (1997) 241.
[19] G.K. Bethke, H.H. Kung, Appl. Catal. A 194 (2000) 43.
[20] R.J.H. Grisel, P.J. Kooyman, B.E. Nieuwenhuys, J. Catal. 191 (2000) 430.
[21] JCPDS Powder Diffraction File, International Centre for Diffraction Data.
[22] N. Lopez, J.K. Norskov, T.V.W. Janssens, A. Carlsson, A. Puig-Molina, B.S. Clausen, J.D. Grunwaldt, J. Catal. 225 (2004) 86.
[23] N. Lopez, J.K. Norskov, J. Am. Chem. Soc. 124 (2002) 11262.
[24] C.P. Vinod, J.W. Niemantsverdriet, B.E. Nieuwenhuys, Appl. Catal. A, in press.
[25] K.-J. Berg, A. Berger, H. Hofmeister, Z. Phys. D 20 (1991) 309.
[26] P. Claus, A. Bruckner, C. Mohr, H. Hofmeister, J. Am. Chem. Soc. 122 (2000) 11430, and references therein.
[27] J.P. Chen, R.T. Yang, Appl. Catal. A 80 (1992) 135.
[28] T. Baba, Y. Inoue, Y. Ono, J. Catal. 159 (1996) 230.
[29] A.C. Gluhoi, N. Bogdanchikova, B.E. Nieuwenhuys, Appl. Catal. A, submitted for publication.
[30] D. Szmigiel, H. Bielawa, M. Kurtz, O. Hinrichsen, M. Muhler, W. Rarog, S. Jodzis, Z. Kowalczyk, L. Znak, J. Zielinski, J. Catal. 205 (2002) 205.